# Supracolloidal Multivalent Interactions and Wrapping of Dendronized Glycopolymers on Native Cellulose Nanocrystals

Johanna Majoinen,[†] Johannes S. Haataja,[†] Dietmar Appelhans,[‡,¶] Albena Lederer,[‡] Anna Olszewska,[§] Jani Seitsonen,[∥] Vladimir Aseyev,[⊥] Eero Kontturi,[§] Henna Rosilo,[†] Monika Österberg,[§] Nikolay Houbenov,*[,†] and Olli Ikkala*[,†]

[†]Department of Applied Physics, Molecular Materials, [§]Department of Forest Products Technology, and [∥]Nanomicroscopy Center, Aalto University (formerly Helsinki University of Technology), FI-00076 Aalto, Espoo, Finland
[‡]Leibniz-Institut für Polymerforschung Dresden e.V., D-01069, Dresden, Germany
[¶]Technische Universität Dresden, D-01062 Dresden, Germany
[⊥]Laboratory of Polymer Chemistry, Department of Chemistry, University of Helsinki, 00014 HY, Helsinki, Finland

**⑤** *Supporting Information*

**ABSTRACT:** Cellulose nanocrystals (CNCs) are high aspect ratio colloidal rods with nanoscale dimensions, attracting considerable interest recently due to their high mechanical properties, chirality, sustainability, and availability. In order to exploit them for advanced functions in new materials, novel supracolloidal concepts are needed to manipulate their self-assemblies. We report on exploring multivalent interactions to CNC surface and show that dendronized polymers (DenPols) with maltose-based sugar groups on the periphery of lysine dendrons and poly(ethylene-*alt*-maleimide) polymer backbone interact with CNCs. The interactions can be manipulated by the dendron generation suggesting multivalent interactions. The complexation of the third generation DenPol (G3) with CNCs allows aqueous colloidal stability and shows wrapping around CNCs, as directly visualized by cryo high-resolution transmission electron microscopy and electron tomography. More generally, as the dimensions of G3 are in the colloidal range due to their ~6 nm lateral size and mesoscale length, the concept also suggests supracolloidal multivalent interactions between other colloidal objects mediated by sugar-functionalized dendrons giving rise to novel colloidal level assemblies.

**S**upramolecular chemistry and molecular self-assembly have been maturing to a rich variety of "bottom-up" approaches for advanced materials using molecular level construction units ranging from low to high molecular weights. Therein the structural information is encoded within the molecules and their balanced mutual interactions, geometrical sizes, and architectures to allow controlled assemblies and functions at molecular length scale.[1] Extension of these concepts to larger colloidal length scale has recently been pursued toward supracolloidal assemblies and new functions.[2] It involves subtleties, as the colloidal level units are more easily prone to aggregation than molecules, they require engineering of stronger and tunable but balanced interactions, and also the control of structural uniformity poses challenges. Several examples can be given on the recent progress: Rod-like metallic nanocrystals combining polymeric functional end groups which lead to colloidal level assemblies and functionalities have been introduced, such as for tunable plasmonics; colloidal assemblies architecturally resembling molecules have been formed; self-assembly between viral capsids and dendrimers have been explored; block-like colloidal level objects have been demonstrated by "living" block copolymer assemblies; and assemblies based on patchy colloids have been described.[2]

Native nanocelluloses have a great promise in materials science as mechanically excellent, sustainable, widely available, and functionalizable 1D colloidal materials,[3] taken that the structures and self-assemblies could be fully mastered and transferred to advanced materials properties. Nanocelluloses can be cleaved from plant cell walls, which constitute the largest source of polymers on the Earth. Due to their native crystalline internal structure consisting of hydrogen-bonded parallel chains, they have extraordinarily high mechanical properties with modulus of ~140 GPa and strength up to GPa range.[4] Two main forms of nanocelluloses can be extracted from plants, both having lateral dimensions in the nanometer range, where the rod-like cellulose nanocrystals (CNCs) have length of ~100−500 nm, while the longer and entangled nanofibrillated celluloses reach micrometers.[3] Nanofibrillated cellulose has been pursued for, e.g., hydrogels, reinforcement of polymer composites, strong and transparent films, and to prepare ductile, lightweight, and functional aerogels.[5] The rod-like CNCs have been used to reinforce polymer blends, templating for chiral assemblies, and they have been decorated with polymer brushes or supramolecular groups for advanced functions, like self-healing material properties.[6] The CNCs are typically prepared by sulphuric acid hydrolysis of macroscopic cellulose fibers, thus leaving anionic sulfate ester groups on the CNC nanorod surface.[3] This allows colloidal stabilization via electrostatics in aqueous medium. The anionic groups have been used to bind cationic surfactants in order to tune the interfacial properties to low polarity medium as well as to prepare layer-by-layer assemblies using anionic CNCs and cationic polyelectrolytes.[7]

Here we show that DenPols with dendritic side groups having maltose-based sugar peripheral units endure tunable generation-

dependent multivalent binding on CNCs resulting in supra-colloidal complexes and colloidal stability. By high-resolution transmission electron microscopy (HR-TEM) we show that G3 undergoes wrapping around the CNCs. Electron tomography (ET) allows to directly visualize the 3D structures, i.e., the wrapping of the G3 around CNC and the chiral twisting of the pristine CNC rods.

This approach was motivated by the following arguments: Even if anionic sulfate esters are available on CNC surfaces for electrostatic binding[7] allowing colloidal stabilization in aqueous media, we searched other complementary interactions toward versatility in supracolloidal nanoconstruction. Considering the available interactions on CNCs, the individual hydroxyl groups on the CNC surface glucose rings lead to only poor hydrogen bonding, as they are neither strong hydrogen-bonding donors nor acceptors. This suggests looking for multivalent binding to glucose rings[8] and hydroxyl groups therein. A hint is given by the strong binding of xyloglucans on nanocelluloses.[9] They have a branched architecture, suppressing excessive mutual aggregation and promoting accessibility of several glucose rings for binding to nanocelluloses.[10] This suggests exploring sugar-functionalized DenPols for tunable binding on nanocelluloses due to their side chain modifications containing branched architecture and tunable number of sugar units at the periphery of the dendrons. In more general, dendrons involving well-defined molecular structures have shown to allow multivalency in a tunable way in other systems upon selecting the peripheral chemical units and the generation properly.[11]

This work deals with water-soluble DenPols consisting of poly(ethylene-*alt*-maleimide) backbones, lysine dendrons of three generations and maltose-based sugar peripheral groups, denoted as G1, G2, G3, accordingly (see Figure 1a for G3, and
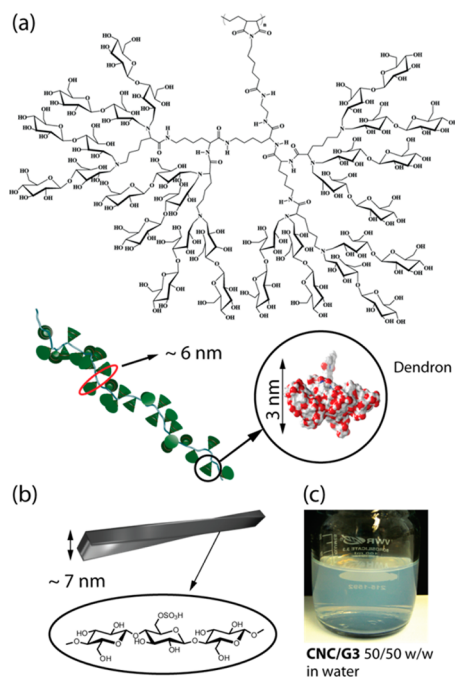
**Figure 1.** (a) Molecular structure of the G3 and a model of one dendritic side chain unit (red color oxygen) assuming full conversion for maltose groups. Schematic illustration of G3 chain with diameter of ~6 nm and (b) of twisted CNC with diameter of 7 nm with surface chemical groups. (c) Aqueous suspension of CNC/G3 50/50 w/w (1.25 mg/mL) suggesting colloidal stability.

Figure S1 for all generations). The synthesis and characterization has been described previously.[12] Molecular weights are $1.3 \times 10^6$, $1.7 \times 10^6$, and $27 \times 10^6$ g/mol for G1, G2, and G3 and each dendron has nominally 4, 8, and 16 maltose-based groups, respectively. The emphasis here is in G3 due to its high binding on CNCs and allowing colloidal stability upon complexing with CNCs (Figure 1c), as will be discussed later. G1 and G2 interactions with CNCs are only discussed as a reference. Figures 2a and S9 show cryogenic HR-TEM micrographs of a 0.1 mg/mL
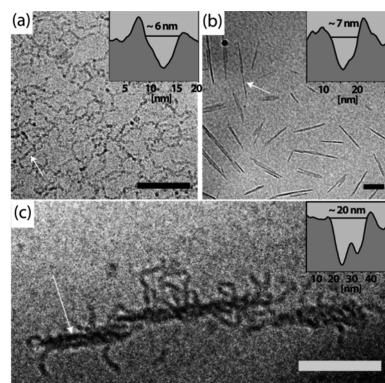
**Figure 2.** Cryo HR-TEM images from (a) G3, (b) CNCs, and (c) CNC/G3 30/70 w/w. The arrows mark the locii for the cross section analysis shown as insets. Scale bars are 100 nm.

aqueous dispersion of G3. The chain adopts a semiflexible worm-like conformation in neutral conditions due to a dense packing of the dendrons along the backbone, as expected also from other dendronized polymers with large side chains.[13] The contrast mapping (inset of Figure 2a) indicates the lateral dimension of ~6 nm, in agreement with the 3 nm dendrons surrounding the polymer backbone (Figure 1a). Calculations suggest the contour length of ~600 nm for G3. Even if the large side-chain steric crowding in G3 causes overall polymer backbone stretching, coiling is still not fully excluded due to possible ethyl maleimide bond rotation in combination with the rearrangements of the dendron side groups. Using dynamic light scattering (DLS), the hydrodynamic radius of aqueous G3 is observed to be ~80 nm (Figure S4), which increases to 140 nm in 3 days incubation time. This increase indicates that G3 ultimately undergoes aggregation with time, as promoted by its very high molecular weight and large physical size. Such aggregation properties are characteristic for colloids, even if G3 is considered as a single macromolecule.

CNCs were prepared by sulphuric acid hydrolysis of Whatman cellulose filter paper, as described previously.[14] Pristine CNCs in water with concentration of 5 mg/mL show essentially clear dispersion, and HR-TEM (Figures 2b, S8) illustrates how CNCs are well-dispersed rod-like objects with an average lateral dimension of ~7 nm and length in the range of 150−250 nm. DLS suggests a hydrodynamic radius of ~50 nm after 3 h without mixing, and an increase to ~90 nm is observed after 3 days incubation time due to some aggregation (Figure S4). We point out that the reported hydrodynamic radii are apparent values and have to be interpreted only qualitatively.

Next, compositions between CNC and DenPols with different weight fractions of each component were prepared, followed by magnetic stirring at room temperature for 24 h. First the colloidal stabilities are studied by visual inspection. Figure S3 shows photographs of samples with the compositions CNC/G1 50/50 w/w, CNC/G2 50/50 w/w, and CNC/G3 50/50 w/w where in

all cases the total CNC/DenPol concentration is 1.25 mg/mL in water. CNC/G1 50/50 w/w undergoes rapid and distinct phase separation from water upon their mixing. CNC/G2 50/50 w/w also shows phase separation but in this case into a more hydrated "fluffy" segregated phase, whereas CNC/G3 50/50 w/w remained essentially clear, just showing a bluish tint (Figures 1c, S3), characteristic to well-dispersed colloidal units. DLS lends further information on the nature of the aqueous mixtures between G3 and CNCs. Except for a narrow composition window in the range of 50−80 % w of CNCs (Figure S4), where large adducts have already grown during the first 3 h of quiescent aging, DLS supports well-dispersed aqueous colloidal level units. Later (Figures 2c, 3b) we directly show that CNCs and G3
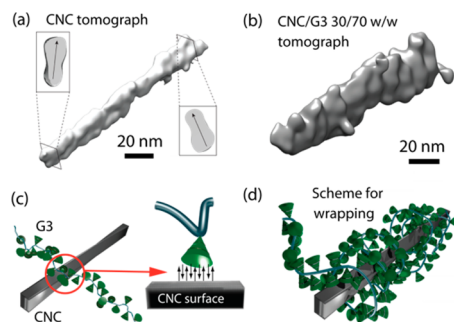


**Figure 3.** ET image of (a) pristine CNC and (b) CNC/G3 30/70 w/w). (c) Schematics of the proposed multivalent interactions between G3 peripheral dendritic units and the CNC surface glucose groups. (d) Schematics for irregular wrapping of G3 on CNC.

interact, and therefore the DLS observation cannot be explained simply by CNCs and G3 dispersing separately. Also, the DLS measurements qualitatively suggest that the hydrodynamic radii of all aqueous combinations of CNC and G3 are larger than those of pure CNC and G3 (Figure S4). Finally, the sizes of the CNC/G3 adducts increase with time after stopping the mixing, like within pristine CNCs and G3. In conclusion, CNC/G3 adducts can form in the colloidal size, forming visually clear aqueous dispersions. By contrast, the corresponding compositions CNC/G1 and CNC/G2 phase segregate from water (Figure S3). This suggests investigating generation dependent binding of DenPols on CNCs. Quartz crystal microbalance with dissipation (QCM-D) shows (Figure S5) qualitatively that the DenPol interactions to CNC surfaces systematically increase from G1 to G3. G1 shows binding reversibility allowing its removal upon aqueous treatment, whereas for G3 the binding is irreversible. For G3, the calculated bonded mass is of 2.53 mg/m$^2$ (Table S2), which is comparable to that of xyloglucan,[15] considered to be state of the art in binding onto cellulose via nonionic interactions. We therefore demonstrate tunability of the binding based on the dendron generation.

Figure 2c shows cryo HR-TEM image of CNC/G3 30/70 w/w (0.1 mg/mL). G3 chains are located close to the CNCs, showing both densely bound regions as well as loose loops, dangling ends, and irregular wrapping of G3 on CNC. More than two G3 loops or ends are shown on the CNC surface suggesting that several G3 molecules may be involved in the assembly. We do not see any naked CNC nanorods, suggesting the attraction between CNCs and G3s to form complexes. We imaged also CNC/G3 complexes as individual fibrillar like assemblies having a tightly wrapped shell of G3 round the CNC core (Figure S10). Larger aggregates are also observed, suggesting CNC/G3 fibrils also

pack as higher order assemblies (Figure S11), which is not surprising based on DLS upon aging (Figure S4).

A still more direct evidence of the wrapping is provided by ET where 3D images are constructed based on a series of differently tilted 2D cryo HR-TEM projections instead of individual 2D projections, which are depicted in classic TEM (Figures 3a,b and S12 for additional graphs). First, Figure 3a shows a tomograph of pristine CNC from a 5 mg/mL aqueous vitrified dispersion having a nanocrystal length of ∼150 nm and lateral dimension in nanometers. Interestingly, ET allows direct visualization of the CNC helicoidal twisting along its longitudinal direction. The proposed scheme of Figure 1b is therefore warranted. This internal twisting within the nanorods is relevant for their cholesteric liquid crystalline assembly and further for their use as chiral templates.[3,6] Figure 3b (also Movie S1) shows a tomograph of an individual CNC/G3 30/70 w/w assembly. An extended composite rod is observed, matching the average CNC length (150−250 nm) but being considerably thicker, due to decoration with cluster-like motifs and protrusions. This supports our model of DenPol wrapping on CNC surface (Figures 3d, 2c).

Wrapping of polymers around colloidal objects has been reported previously for, e.g., carbon nanotubes and montmorillonite nanosheets, based on TEM and AFM studies.[16] Therein, the small lateral dimension of the wrapping polymers poses challenges to clearly resolve the structures at the individual polymer level. By contrast, in the present case the large diameter of the G3 DenPol allows to resolve the wrapping processes toward individual polymer resolution.

Next, we will comment on the nature of the binding of CNCs with DenPols and the colloidal stabilities, which can involve a subtle set of interactions. Figure 1a illustrates that in G3 there is nominally a set of 16 maltose-based groups on the periphery. The nature of the interactions between G3 and CNC could not be ascertained using Fourier transform infrared spectra (Figure S13). In general, taking into account the chemical structure of cellulose involving chains of 1→4 joined glucose-units and that of the peripheral groups in DenPols, which involve highly available sugar unit, it is expected that multivalent interactions between glucose units can take place. Such interactions can involve combinations of hydrogen bonds as well as potential stackings (Figure 3c). Note, that individual glucose units provide only weak binding on cellulose, whereas several glucose units are needed to promote adsorption.[17] Therefore, generation-dependent interaction on cellulose is foreseen, as G3 provides larger number of sugar groups to facilitate the interactions. On the other hand, the preparation of CNCs by sulphuric acid hydrolysis causes that approximately every tenth surface glucose ring involves an acidic sulfate ester group.[3] The sugar-capped lysine dendrons involve tertiary amines in their scaffolds (Figures 1a, S1) which may possess a weak cationic charge at neutral pH.[12] Therefore, electrostatic interactions are also possible. However, under neutral conditions the sugar functionalities are essential, as shown by QCM-D measurement (Figure S7): A reference material of G3 without sugar periphery (Figure S6) does not bind onto CNC. This suggests that in the sugar functionalized G3, the tertiary amines are sterically hindered behind the sugar groups (Figure S2), reducing the strength of the potential ionic interaction. In G1 and G2 this hindrance is less, and stronger ionic interactions to CNCs cannot be excluded. Beyond providing a controlled number of interacting glucoses, the branched architecture of sugar decorated dendrons also effectively suppresses excessive aggregation, which easily would

take place upon linear cellulose chains. Different branched architectures are observed in xyloglucans, known to adsorb strongly on cellulose.[9] Finally, a comment can be given on the improved aqueous colloidal stability in mixtures of CNCs and G3. Taken that the dendrons surround the G3 polymer backbone essentially in a cylindrically symmetric manner (Figure 1a), at the periphery of the CNC/G3 complex there is a dense set of sugar dendrons, mediating interaction also toward the external aqueous phase (Figure 3d). We postulate that such a dense set of hydrophilic sugar moieties in CNC/G3 allows water dispersibility. In lower generations, phase segregation was observed. A potential explanation is given by formation of more probable ionic interactions between the CNCs and lower generation DenPols as well as the less dense set of hydrophilic sugar groups.

In summary, we show that polymers equipped with a dense set of peripheral maltose-based sugar groups allow multivalent binding on native CNCs, where wrapping is visualized directly using cryo HR-TEM and ET. The dendritic architecture provides a feasible approach to design binding on nanocelluloses and more general on cellulose surfaces. Due to the dimensions, G3 can also be considered as a colloidal object. Therefore, the present findings suggest even routes for supracolloidal assemblies, i.e., self-assemblies between colloidal level objects. We foresee that the dendronized glucose-based approaches allow a generic route and great versatility for interacting with nanocellulose, where such moieties could be connected to nanoparticles, block copolymers, and surfaces. Taken the growing importance of colloidal constructs and native nano-celluloses as mechanically strong and chiral colloidal level fibers, the glucose-decorated dendron motifs open new platforms for supracolloidal assemblies and to engineer novel properties toward applications in science and industry.

## ■ ASSOCIATED CONTENT

### Ⓢ Supporting Information

Characterization details and data. This material is available free of charge via the Internet at http://pubs.acs.org.

## ■ AUTHOR INFORMATION

### Corresponding Authors

Nikolay.Houbenov@aalto.fi
Olli.Ikkala@aalto.fi

### Notes

The authors declare no competing financial interest.

## ■ ACKNOWLEDGMENTS

## ■ REFERENCES

(1) Ozin, G. A.; A. C. Arsenault, A. C. *Nanochemistry; A Chemical Approach for Nanomaterials*, Royal Society of Chemistry: Cambridge, 2005.
(2) (a) Liu, K.; Nie, Z.; Zhao, N.; Li, W.; Rubinstein, M.; Kumacheva, E. *Science* **2010**, *329*, 197. (b) Wang, Y.; Wang, Y.; Breed, D. R.; Manoharan, V. N.; Feng, L.; Hollingsworth, A. D.; Weck, M.; Pine, D. J. *Nature* **2012**, *491*, 51. (c) Kostiainen, M. A.; Kasyutich, O.; Cornelissen, J. J. L. M.; Nolte, R. J. M. *Nat. Chem.* **2010**, *2*, 394. (d) Wang, X.; Guerin, G.; Wang, H.; Wang, Y.; Manners, I.; Winnik, M. A. *Science* **2007**, *317*, 644. (e) Gröschel, A. H.; Felix H. Schacher, F. H.; Schmalz, H.; Oleg V. Borisov, O. V.; Zhulina, E. B.; Walther, A.; Müller, A. H. E. *Nat. Commun.* **2012**, *3*, 710.
(3) (a) Klemm, D.; Kramer, F.; Moritz, S.; Lindstrom, T.; Ankerfors, M.; Gray, D.; Dorris, A. *Angew. Chem., Int. Ed.* **2011**, *50*, 5438. (b) Habibi, Y.; Lucia, L. A.; Rojas, O. J. *Chem. Rev.* **2010**, *110*, 3479. (c) Lin, N.; Huang, J.; Dufresne, A. *Nanoscale* **2012**, *4*, 3274.
(4) (a) Iwamoto, S.; Kai, W. H.; Isogai, A.; Iwata, T. *Biomacromolecules* **2009**, *10*, 2571. (b) Saito, T.; Kuramae, R.; Wohlert, J.; Berglund, L. A.; Isogai, A. *Biomacromolecules* **2013**, *14*, 248.
(5) (a) Pääkkö, M.; Ankerfors, M.; Kosonen, H.; Nykänen, A.; Ahola, S.; Österberg, M.; Ruokolainen, J.; Laine, J.; Larsson, P. T.; Ikkala, O.; Lindström, T. *Biomacromolecules* **2007**, *8*, 1934. (b) Nogi, M.; Iwamoto, S.; Nakagaito, A. N.; Yano, H. *Adv. Mater.* **2009**, *21*, 1595. (c) Henriksson, M.; Berglund, L. A.; Isaksson, P.; Lindström, T.; Nishino, T. *Biomacromolecules* **2008**, *9*, 1579. (d) Pääkkö, M.; Silvennoinen, R.; Vapaavuori, J.; Nykänen, A.; Ankerfors, M.; Kosonen, H.; Ruokolainen, J.; Lindström, T.; Berglund, L. A.; Ikkala, O. *Soft Matter* **2008**, *4*, 2492.
(6) (a) Capadona, J. R.; van den Berg, O.; Capadona, L. A.; Schroeter, M.; Rowan, S. J.; Tyler, D. J.; Weder, C. *Nat. Nanotechnol.* **2007**, *2*, 765. (b) Lin, N.; Huang, J.; Dufresne, A. *Nanoscale* **2012**, *4*, 3274. (c) Shopsowitz, K. E.; Qi, H.; Hamad, W. Y.; MacLachlan, M. J. *Nature* **2010**, *468*, 422. (d) Majoinen, J.; Walther, A.; McKee, J. R.; Kontturi, E.; Aseyev, V.; Malho, J.-M.; Ruokolainen, J.; Ikkala, O. *Biomacromolecules* **2011**, *12*, 2997. (e) Zoppe, J. O.; Habibi, Y.; Rojas, O. J.; Venditti, R. A.; Johansson, L.-S.; Efimenko, K.; Osterberg, M.; Laine, J. *Biomacromolecules* **2010**, *11*, 2683. (f) Kloser, E.; Gray, D. G. *Langmuir* **2010**, *16*, 13450. (g) Biyani, M. V.; Foster, E. J.; Weder, C. *ACS Macro Letters* **2013**, *2*, 236.
(7) (a) Salajkova, M.; Berglund, L. A.; Zhou, Q. *J. Mat. Chem.* **2012**, *22*, 19798. (b) Cranston, E. D.; Gray, D. G. *Biomacromolecules* **2006**, *7*, 2522. (c) Podsiadlo, P.; Choi, S-Y; Shim, B.; Lee, J.; Cuddihy, M.; Kotov, N. A. *Biomacromolecules* **2005**, *6*, 2914.
(8) Wolfenden, M. L.; Cloninger, M. J. *Bioconjugate Chem.* **2006**, *17*, 958.
(9) (a) Jean, B.; Heux, L.; Dubreuil, F.; Chambat, G.; Cousin, F. *Langmuir* **2009**, *25*, 3920. (b) Zhou, Q.; Rutland, M. W.; Teeri, T. T.; Brumer, H. *Cellulose* **2007**, *14*, 625.
(10) (a) Lopez, M.; Bizot, H.; Chambat, G.; Marais, M-F; Zykwinska, A.; Ralet, M-C; Driguez, H.; Buleon, A. *Biomacromolecules* **2010**, *11*, 1417. (b) Hanus, J.; Mazeau, K. *Biopolymers* **2006**, *82*, 59.
(11) (a) Rosen, B. M.; Wilson, C. J.; Wilson, D. A.; Peterca, M.; Imam, M. R.; Percec, V. *Chem. Rev.* **2009**, *109*, 6275. (b) Röglin, L.; Lempens, E. H. M.; Meijer, E. W. *Angew. Chem., Int. Ed.* **2011**, *50*, 102.
(12) Boye, S.; Appelhans, D.; Boyko, V.; Zschoche, S.; Komper, H.; Friedel, P.; Formanek, P.; Janke, A.; Voit, B. I.; Lederer, A. *Biomacromolecules* **2012**, *13*, 4222.
(13) Zhang, B.; Wepf, R.; Fischer, K.; Schmidt, M.; Besse, S.; Lindner, P.; King, B. T.; Sigel, R.; Schurtenberger, P.; Talmon, Y.; Ding, Y.; Kröger, M.; Halperin, A.; Schlüter, A. D. *Angew. Chem., Int. Ed. Engl.* **2011**, *50*, 737.
(14) Edgar, C. D.; Gray, D. G. *Cellulose* **2003**, *10*, 299.
(15) Ahola, S.; Myllytie, P.; Österberg, M.; Teerinen, T.; Laine, J. *Bioresources* **2008**, *3*, 1315.
(16) (a) Kim, O.-K.; Je, J.; Baldwin, J. W.; Kooi, S.; Pehrsson, P. E.; Buckley, L. J. *J. Am. Chem. Soc.* **2003**, *125*, 4426. (b) Didenko, V. V.; Moore, V. C.; Baskin, D. S.; Smalley, R. E. *Nano Lett.* **2005**, *8*, 1563. (c) Satake, A.; Miyajima, Y.; Kobuke, Y. *Chem. Mater.* **2005**, *17*, 716. (d) Zhang, F.; Zhang, H.; Zhang, Z.; Chen, Z.; Qun, X. Q. *Macromolecules* **2008**, *41*, 4519. (e) Kim, J. K.; Kataoka, M.; Kumagai, A.; Nishijima, H.; Amano, Y.; Kim, Y. A.; Endo, M. *ChemSusChem* **2011**, *4*, 1595. (f) Walther, A.; Bjurhager, I.; Malho, J.-M.; Ruokolainen, J.; Pere, J.; Berglund, L. A.; Ikkala, O. *Nano Lett.* **2010**, *10*, 2742.
(17) Yokota, S.; Ohta, T.; Kitaoka, T.; Ona, T.; Wariishi, H. *Sen'i Gakkaishi* **2009**, *8*, 212.